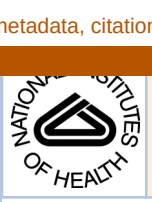

Published in final edited form as:

J Magn Reson. 2003 February ; 160(2): 85–90.

Dynamic nuclear polarization at 9T using a novel 250GHz gyrotron microwave source

V.S. Bajaj[a], **C.T. Farrar**[a], **M.K. Hornstein**[b], **I. Mastovsky**[b], **J. Vieregg**[b,1], **J. Bryant**[a], **B. Eléna**[a,2], **K.E. Kreischer**[b,3], **R.J. Temkin**[b], and **R.G. Griffin**[a,*]

[a] Francis Bitter Magnet Laboratory, Department of Chemistry, Massachusetts Institute of Technology, 170 Albany Street, Room NW 14-3220, Cambridge, MA 02139, USA

[b] Plasma Science and Fusion Center, Massachusetts Institute of Technology, Cambridge, MA 02139, USA

Abstract

In this communication, we report enhancements of nuclear spin polarization by dynamic nuclear polarization (DNP) in static and spinning solids at a magnetic field strength of 9T (250 GHz for $g = 2$ electrons, 380 MHz for ^{1}H). In these experiments, ^{1}H enhancements of up to 170 ± 50 have been observed in 1-^{13}C-glycine dispersed in a 60:40 glycerol/water matrix at temperatures of 20 K; in addition, we have observed significant enhancements in ^{15}N spectra of unoriented *pf1*-bacteriophage. Finally, enhancements of ~17 have been obtained in two-dimensional ^{13}C–^{13}C chemical shift correlation spectra of the amino acid U-^{13}C, ^{15}N-proline during magic angle spinning (MAS), demonstrating the stability of the DNP experiment for sustained acquisition and for quantitative experiments incorporating dipolar recoupling. In all cases, we have exploited the thermal mixing DNP mechanism with the nitroxide radical 4-amino-TEMPO as the paramagnetic dopant. These are the highest frequency DNP experiments performed to date and indicate that significant signal enhancements can be realized using the thermal mixing mechanism even at elevated magnetic fields. In large measure, this is due to the high microwave power output of the 250 GHz gyrotron oscillator used in these experiments.

1. Introduction

During the last decade, a considerable variety of NMR techniques have been developed to constrain molecular structure in the solid state. In order to obtain site-specific resolution, these involve either uniaxial orientation of the sample with respect to the static magnetic field [1] or magic angle spinning (MAS) [2]. In the latter case, anisotropic dipolar and chemical shift interactions which encode structural parameters are modulated by the sample spinning and must be re-introduced to yield useful information. In particular, there is now a multiplicity of well-developed homonuclear and heteronuclear dipolar recoupling techniques [3,4] useful as mixing sequences in chemical shift correlation spectroscopy [5], for distance measurements [6], and for the determination of torsion angles [7-11]. Recently, a complete atomic-resolution structure determined using these techniques has been reported in the literature [12].

* Corresponding author. Fax: 1-617-253-5405. rgg@mit.edu, griffin@ccnmr.mit.edu (R.G. Griffin)..

[1] Present address: Department of Physics, University of California, Berkeley, CA 94720, USA.

[2] Present address: LSIM, ENS-Lyon, 69364, Lyon, FRANCE.

[3] Present address: Vacuum Electronics Research, Development and Engineering, Northrup-Grumman Corporation, 600 Hicks Road, Rolling Meadows, IL 60008, USA.

In all cases, the applicability of these methods to larger systems and those in low abundance is currently limited by the necessity to directly observe signals of low gyromagnetic ratio (γ) nuclei, such as ^{13}C, ^{15}N, and ^{31}P, whose spectra are well-resolved. The indirect detection of dilute spin spectra through the more sensitive ^{1}H spins has not yet become generally practical in the solid state, due to strong homonuclear couplings among the protons [13-15]. As a result, solid state NMR is less sensitive by two or three orders of magnitude per unit time than solution state NMR. This inherent low sensitivity is a limiting factor in the application of multidimensional NMR methods to biological systems.

As a means to increase the sensitivity of these experiments, we have previously employed dynamic nuclear polarization (DNP) to enhance NMR signals in both static and rotating solids at 5T [16-19]. DNP involves the irradiation of a coupled electron-nuclear spin system in the neighborhood of the electron Larmor frequency. According to a variety of polarization transfer mechanisms which rely on electron-nuclear hyperfine couplings alone (e.g., solid effect), or electron dipolar couplings in addition to hyperfine couplings to the nuclei (e.g., thermal mixing), nuclear signal enhancements on the order of γ_e/γ_N (~660 for ^{1}H nuclei and ~2600 for ^{13}C nuclei), are possible. In general, these experiments are conducted at low temperatures in order to attenuate competing spin–lattice relaxation processes which would otherwise compromise the polarization transfer efficiency. In earlier work, we have achieved ^{1}H signal enhancements ranging from 50 to 400 at a magnetic field of 5T. However, it is desirable to apply DNP at higher fields (9–18 T) where NMR is commonly performed.

In this communication, we present preliminary results which illustrate the successful application of DNP at a magnetic field of 9 T in both static and rotating solids. In all cases, samples were dissolved or dispersed in frozen solutions of 60% glycerol and 40% water, and the source of electron polarization was the nitroxide radical 4-amino-TEMPO. We have obtained static ^{1}H thermal mixing DNP enhancements of up to 170 ± 50 for the amino acid 1-^{13}C-glycine at 20 K, and an enhancement of ~40 in an unoriented sample of U-^{15}N-*pf1*-bacteriophage. Further, we have recorded two-dimensional ^{13}C–^{13}C chemical shift correlation spectra of U-^{13}C, ^{15}N-proline in magic angle spinning dipolar recoupling experiments at 98–100 K, with a DNP enhancement of 17.

2. Thermal mixing DNP at high fields

For systems in which the homogeneous EPR line width approaches the magnitude of the nuclear Larmor frequency, an energy conserving three-spin process is operative. Here, an allowed electron–electron mutual spin flip is accompanied by a nuclear spin flip; for the case of a non-equilibrium polarization among the electrons, this mode of relaxation can lead to the generation of enhanced nuclear polarization, a process which is referred to as thermal mixing. Thermal mixing is conventionally treated by a spin thermodynamic formalism in which the Hamiltonian for the coupled three-spin system is decomposed into several quasi-invariants of the motion, each of which has a distinct spin temperature. These are: the electron Zeeman spin reservoir (in the rotating frame), the electron spin–spin interaction reservoir, and the nuclear Zeeman bath. As shown by Provotorov [20], the electron Zeeman and spin–spin interaction reservoirs are in thermodynamic equilibrium when microwave radiation is applied. Off-resonance irradiation of the EPR line produces a non-equilibrium polarization state that is equivalent to cooling of the electron spin–spin interaction reservoir. This spin–spin interaction reservoir is in thermal contact with the nuclear Zeeman system through the aforementioned three-spin process involving two electron spins and one nuclear spin, and so off-resonance irradiation of the EPR line can also produce a cooling of the nuclear Zeeman reservoir.

Treatments based on perturbation theory or a relaxation approach [21,22] both require that the homogeneous EPR line width (δ) be greater than the nuclear Larmor frequency (ω_n) for the thermal mixing DNP enhancement to be appreciable. If the enhanced nuclei are protons in an organic solid, the polarization is redistributed across the sample by spin diffusion which is fast on the time scale of the DNP experiment. In the limit of fast spin diffusion and under the approximation of a homogeneous electron line shape, Wind et al. [23] have derived an expression for the dependence of the enhancement (ε) on the various experimental parameters, given by Eq. (1).

$$\varepsilon \propto \frac{\gamma_e}{\gamma_n}\frac{N_e^2}{\delta^2}\left(\frac{B_{1e}^2}{B_0}\right)T_{1n}T_{1e}. \quad (1)$$

Here B_{1e} is the microwave field strength, B_0 is the static magnetic field strength, N_e is the concentration of electrons, δ is the homogeneous EPR line width, and T_{1n} and T_{1e} are, respectively, the nuclear and electron spin–lattice relaxation times.

The assumptions inherent to this formulation are not satisfied under the conditions of the experiments described here. In particular, at high magnetic fields (e.g., 9 T), the EPR spectra of the nitroxide radicals used as polarizing agents in DNP experiments are inhomogeneously broadened by the g-anisotropy. The result is that there cannot be a single Zeeman spin temperature assigned to the electrons, and that equilibration of the nuclear and electron Zeeman reservoirs does not necessarily proceed through the dipolar system of the electrons. Farrar et al. [24] have recently presented a phenomenological interpretation of thermal mixing DNP at high fields which relaxes these assumptions. In the limit of a large electron concentration, this treatment suggests that electron cross relaxation, which is fast compared to the spin–lattice relaxation, can indirectly mediate spin temperature equilibration, effectively rendering the electron interactions homogeneous on the time-scale of the experiment. This treatment together with experimental data demonstrate that Eq. (1) is qualitatively valid. Although Eq. (1) suggests an inverse dependence of the DNP enhancement on the static magnetic field, we have been able to compensate for this dependence in our experiments, as follows:

1. Far from saturation, the DNP enhancement qualitatively scales as B_{1e} and so the high output power of the 250 GHz gyrotron oscillator used in these experiments results in a large enhancement.
2. Through manipulation of the sample temperature, nuclear spin–lattice relaxation has been attenuated. Thus, significant enhancements can be realized at temperatures of 10–20 K. Although the MAS experiments are currently conducted near 100 K, significant signal enhancements are also observed in that regime.
3. A large radical concentration (60mM) was used in these experiments, with the result that electron–electron cross-relaxation is enhanced, and the thermal mixing DNP efficiency improved accordingly.

3. 250 GHz gyrotron oscillator

In all experiments presented here, the source of microwave radiation was a 250GHz gyrotron (cyclotron resonance maser) designed for DNP experiments [25]. This instrument is capable of sustained (72–96 h) operation at output powers of 10–15 W, which results in approximately 3–4 W of microwave power at the sample. The output power of the gyrotron is regulated to within 1% through a proportional control loop.

In a probe designed for static DNP experiments, microwave power from the 250GHz gyrotron oscillator is coupled to the sample directly through an over-moded circular waveguide immediately below the NMR coil; no microwave resonant structure was used. Low temperature operation is achieved through a continuous flow of either nitrogen or helium gas near their respective boiling points. In the case of helium gas, dielectric breakdown limited the strength of ^{1}H decoupling which could be applied. MAS experiments were performed using a triple-channel transmission line probe incorporating a microwave waveguide and a 4mm stator. Cryogenic operation was achieved by passing the drive and bearing nitrogen gas through a heat exchanger operating at liquid nitrogen temperatures. The temperature and pressure of the drive and bearing gas are actively regulated using multiple control loops implemented in software, with the result that the temperature is stable to within 1K and the MAS frequency to within 5Hz for extended operating periods. Data acquisition and processing were accomplished using a custom-designed spectrometer and processing software (courtesy Dr. D.J. Ruben). Further details of the gyrotron and DNP spectrometer will be provided in a subsequent publication.

4. DNP CP of static samples

In the case of static samples, the sample and paramagnetic dopant were dissolved in a solution of glycerol and water and transferred to a 4mm quartz tube without further degassing. Provided that freezing is sufficiently rapid, the matrix forms a glass at the temperature of these experiments.

Experimental data were acquired using cross-polarization with continuous microwave irradiation (Fig. 1). The electron resonance offset (vide infra) was set to maximize the ^{1}H thermal mixing DNP enhancement. Accordingly, the reported enhancements are enhancements of the ^{1}H polarization detected indirectly through the dilute spins (^{13}C or ^{15}N). Previous results at 5T demonstrate that proton polarization is homogeneously distributed through the sample by rapid proton spin diffusion on the timescale of the experiment [26]. Further, we have observed in these studies that the directly and indirectly detected ^{1}H enhancements are identical. A representative static spectrum of 1-^{13}C-glycine is shown in Fig. 2. The DNP enhancement of 170 ± 50 at 20 K was achieved with a radical concentration of 80 mM, and an enhancement of approximately 40 was also obtained in a sample of *pf1*-bacteriophage doped with TEMPO at 60mM concentration (not shown). The enhancements obtained at 9T from the glycine sample (Fig. 2) are almost identical in magnitude to previous results obtained at 5T [16], indicating that the inverse dependence of the thermal mixing enhancement on the static magnetic field has been overcome under the conditions of these experiments.

In general, the DNP enhancement is strongly dependent upon the position of irradiation relative to the electron resonance. Since the gyrotron oscillator is fixed in frequency, the static magnetic field was swept from 89,000 to 89,500G (a Zeeman range which encloses the entire EPR line shape) in order to maximize the enhancement. In Fig. 3, we show the field dependence of the DNP enhancement in a static sample of 1-[^{13}C]glycine doped with 60 mM 4-amino-TEMPO at 90 K together with a simulated EPR spectrum at 250 GHz. Since these spectra were acquired at a higher temperature and lower radical concentration than those in Fig. 2, the DNP enhancement is lower. On the basis of these results, we have assigned the DNP effect observed here to the thermal mixing mechanism. In particular, the maximum DNP enhancement occurs within the EPR line shape, a fact which is consistent with the excitation of allowed EPR transitions and not forbidden ones.

5. DNP MAS experiments at 9 T

A variety of techniques have been successfully applied to produce sensitivity enhancements in MAS spectra. These are based upon indirect detection of low γ nuclei during fast MAS [13,14], improved multiple pulse decoupling [15], or a combination of both [27]. Thermal mixing DNP is complementary to these methods, as the dynamics of electron nuclear polarization transfer do not involve any coherent manipulation of the nuclear spins. Further, DNP can produce signal enhancements of a few orders of magnitude. For the DNP/MAS experiments presented here, the sample, consisting of U-^{13}C, ^{15}N-proline in a 60% glycerol matrix doped with 60mM TEMPO, was loaded into a 4mM sapphire rotor while still in the liquid state and frozen in situ. In Fig. 5, we show two-dimensional chemical shift correlation spectra of proline taken using: (a) SPC5 homonuclear double-quantum mixing [28] and (b) proton-driven spin diffusion (see Fig. 4). In both cases, the DNP enhancement was approximately 17, and the microwave output power was stable to within 1%.

6. Conclusions

Using a 250GHz gyrotron microwave source, we have obtained signal enhancements of up to 170 ± 50 at a magnetic field strength of 9T. These results illustrate that it is feasible to manipulate experimental conditions including temperature, concentration and nature of paramagnetic dopant, and microwave power to obtain large enhancements of nuclear spin polarization even in elevated magnetic fields. A detailed study of these experimental parameters is currently in progress, and we are currently constructing a 460GHz second harmonic gyrotron oscillator for DNP experiments at 16.5 T (700 MHz ^{1}H) [29]. Finally, the routine incorporation of DNP into multidimensional correlation experiments, and, in particular, dipolar recoupling experiments, is now possible, and we are currently pursuing applications to the quantitative spectroscopy of biological systems.

Acknowledgments

We thank Dr. Melanie Rosay and Dr. Nathan Astroff for numerous helpful discussions during the course of this research, and Dr. David Ruben, Peter Allen, Ajay Thakkar, Bill Mulligan, and Dr. Chris Turner for advice and technical support. VSB acknowledges receipt of an NSERC PGS Fellowship. This research was supported by the National Institutes of Health through Grants GM-35382, GM-55327 and RR-00995.

References

1. Opella SJ. NMR and membrane proteins. Nat. Struct. Biol 1997;4:845–848. [PubMed: 9377156]
2. Griffin RG. Structural studies of biological solids: magic angle spinning and dipolar recoupling. Nat. Struct. Biol., NMR Suppl 1998:508–512.
3. Bennett AE, Griffin RG, Vega S. Recoupling of homo- and heteronuclear dipolar interactions in rotating solids. NMR Basic Princ. Prog 1994;33
4. Dusold S, Sebald A. Dipolar recoupling under magic angle spinning conditions. Annu. Rep. NMR Spectrosc 2000:185–264.
5. Baldus M. Correlation experiments for assignment and structure elucidation of immobilized polypeptides under magic angle spinning. Prog. Nucl. Magn. Reson. Spectrosc 2002;41:1–47.
6. Jaroniec CP, Tounge BA, Herzfeld J, Griffin RG. Frequency selective heteronuclear dipolar recoupling in rotating solids: accurate ^{13}C–^{15}N distance measurements in uniformly ^{13}C, ^{15}N-labebed peptides. J. Am. Chem. Soc 2001;123:3507–3519. [PubMed: 11472123]
7. Schmidt-Rohr K. Torsion angles in polymers. Macromolecules 1996;29:3975–3981.
8. Feng X, Lee YK, Sandstroöm D, Edén M, Maisel H, Sebald A, Levitt MH. Direct determination of a molecular torsional angle by solid-state NMR. Chem. Phys. Lett 1996;257:314–320.

9. Hong M, Gross JD, Griffin RG. Site-resolved determination of peptide torsion angle phi from the relative orientations of backbone N–H and C–H bonds by solid-state NMR. J. Phys. Chem. B 1997;101:5869–5874.
10. Costa PR, Gross JD, Hong M, Griffin RG. Solid-state NMR measurement of ψ in peptides: a NCCN 2Q-heteronuclear local field experiment. Chem. Phys. Lett 1997;280:95.
11. Ladizhansky V, Veshtort M, Griffin RG. NMR determination of the torsion angle ψ in α-helical peptides and proteins: the HCCN dipolar correlation experiment. J. Magn. Reson 2002;154:317–324. [PubMed: 11846590]
12. Rienstra CM, Tucker-Kellogg L, Jaorniec CP, Hohwy M, Reif B, McMahon M, Tidor B, Lozano-Perez T, Griffin RG. De novo determination of peptide structure with solid-state MAS NMR spectroscopy. Proc. Natl. Acad. Sci 2002;99:10260–10265. [PubMed: 12149447]
13. Ishii Y, Tycko R. Sensitivity enhancement in solid state 15N NMR by indirect detection with high-speed magic angle spinning. J. Magn. Reson 2000;142:199. [PubMed: 10617453]
14. Reif B, Jaroniec CP, Rienstra CM, Hohwy M, Griffin RG. ^{1}H–^{1}H correlation spectroscopy and distance measurements in a deuterated peptide. J. Magn. Reson 2001;151:320–327. [PubMed: 11531354]
15. Vinogradov E, Madhu PK, Vega S. Proton spectroscopy in solid state nuclear magnetic resonance with windowed phase modulated Lee–Goldburg decoupling sequences. Chem. Phys. Lett 2002;354:3–4. 193–202.
16. Gerfen GJ, Becerra LR, Hall DA, Singel DJ, Griffin RG. High frequency (140 GHz) dynamic nuclear polarization: polarization transfer to a solute in frozen aqueous solution. J. Chem. Phys 1995;102:9494–9497.
17. Hall DA, Maus DA, Gerfen GJ, Inati SJ, Beccera LR, Dahlquist FW, Griffin RG. Polarization-enhanced NMR spectroscopy of biomolecules in frozen solution. Science 1997;276:930–932. [PubMed: 9139651]
18. Weis V, Bennati M, Rosay M, Bryant JA, Griffin RG. High-field DNP and ENDOR with a novel multiple-frequency resonance structure. J. Magn. Reson 1999;140:293–299. [PubMed: 10479576]
19. Rosay M, Weis V, Kreischer K, Temkin R, Griffin RG. Two dimensional ^{13}C–^{13}C correlation spectroscopy with magic angle spinning and dynamic nuclear polarization. J. Am. Chem. Soc 2002;124:3214–3215. [PubMed: 11916398]
20. Provotorov BN. Magnetic resonance saturation in crystals. Sov. Phys. JETP 1962;14:1126.
21. Wenckebach WT, Swanenburg TJB, Poulis NJ. Thermodynamics of spin systems in paramagnetic crystals. Phys. Rep 1974;14:181–255.
22. Duijvestijn MJ, Wind RA, Smidt J. A quantitative investigation of the dynamic nuclear polarization effect by fixed paramagnetic centra of abundant and rare spins in solids at room temperature. Physica B 1986;138:147–170.
23. Wind RA, Duijvestijn MJ, van der Lugt C, Manenschijn A, Vriend J. Applications of dynamic nuclear polarization in ^{13}C NMR in solids. Prog. Nucl. Magn. Reson. Spectrosc 1985;17:33–67.
24. Farrar CT, Hall DA, Gerfen GJ, Inati SJ, Griffin RG. Mechanism of dynamic nuclear polarization in high magnetic fields. J. Chem. Phys 2001;114:4922–4933.
25. Kreischer, KE.; Farrar, CT.; Griffin, RG.; Temkin, RJ.; Vieregg, J. The development of a 250 GHz CW gyrotron for EPR and NMR spectroscopy; Proc. 24th Int. Conf. Infrared and Millimeter Waves, Paper IU-A3; 1993.
26. Rosay M, Zeri A, Astrof NS, Opella SJ, Herzfeld J, Griffin RG. Sensitivity enhanced NMR of biological solids: dynamic nuclear polarization of Y21M fd bacteriophage and purple membrane. J. Am. Chem. Soc 2001;123:1010–1011. [PubMed: 11456650]
27. Madhu PK, Zhao X, Levitt MH. High-resolution ^{1}H NMR in the solid state using symmetry-based pulse sequences. Chem. Phys. Lett 2001;346:142–148.
28. Hohwy M, Rienstra CM, Jaroneic CP, Griffin RG. Fivefold symmetric homonuclear dipolar recoupling in rotating solids: application to double quantum spectroscopy. J. Chem. Phys 1999;110:7983.
29. Hornstein MK, Bajaj VS, Griffin RG, Kreischer KE, Mastovsky I, Shapiro MA, Temkin RJ. Design of a 460 GHz second harmonic gyrotron oscillator for use in dynamic nuclear polarization. Int. Conf. Infrared and Millimeter Waves. 2002

30. Budil, D.; Earle, KA.; Lynch, WB.; Freed, JH. Advanced EPR: Applications in Biology and Chemistry. Hoff, AJ., editor. Elsevier; Amsterdam: 1989.

31. Rienstra CM, Hohwy M, Hong M, Griffin RG. 2D and 3D $^{15}N^{13}C^{13}C$ NMR chemical shift correlation spectroscopy of solids: assignment of MAS spectra of peptides. J. Am. Chem. Soc 2000;122:10979–10990.

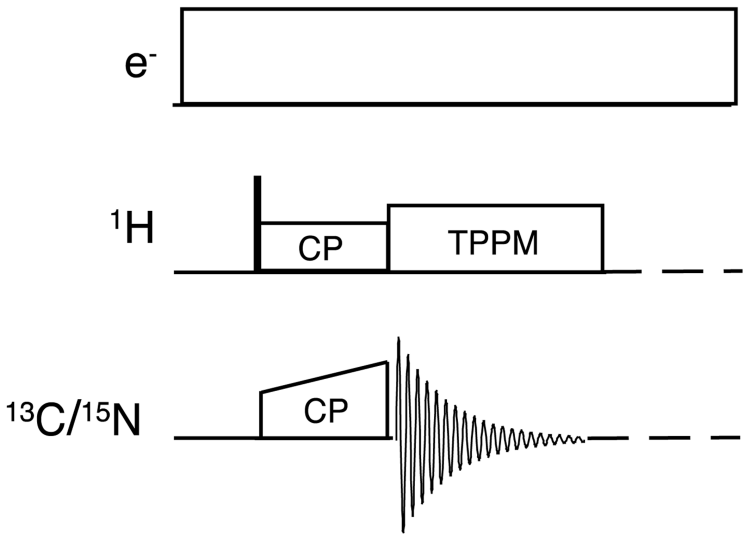

Fig. 1.
Cross-polarization with continuous microwave irradiation. In all cases, the electron resonance offset was set to maximize the ^{1}H enhancement.

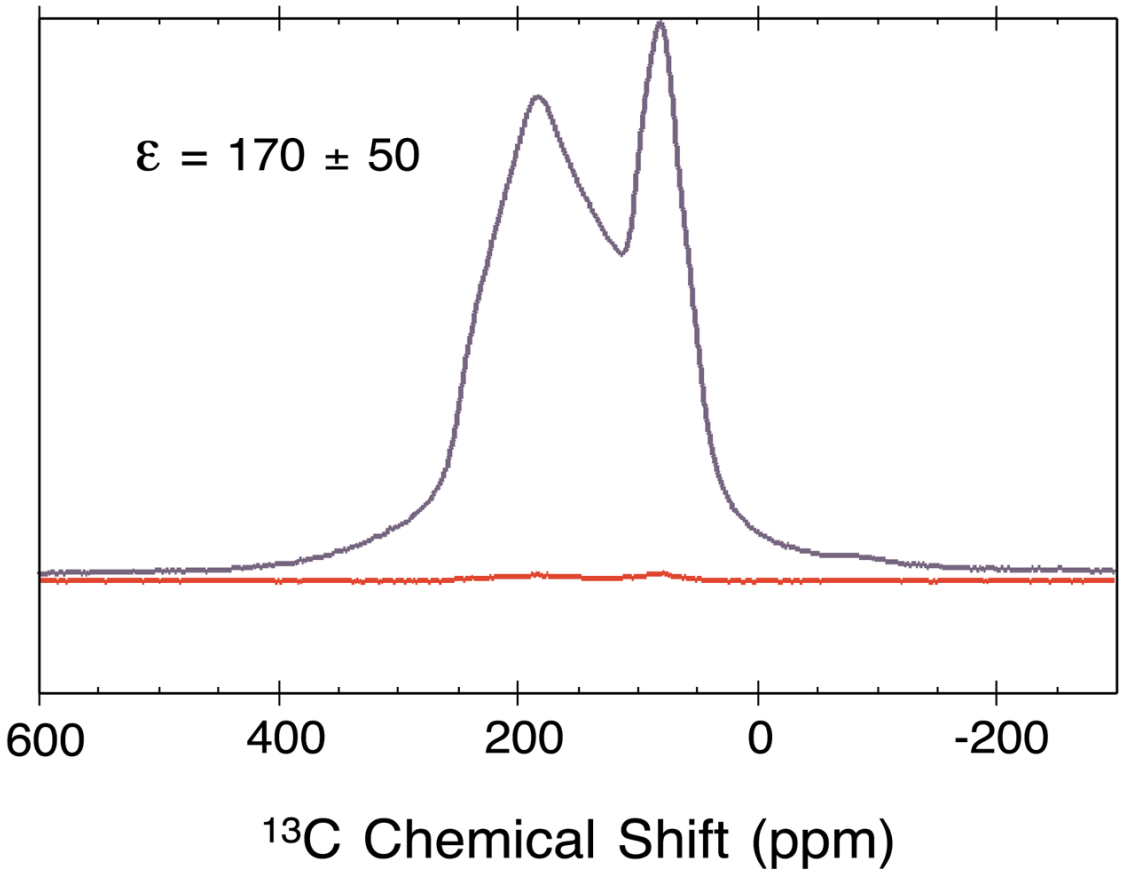

Fig. 2.

DNP CP spectra of static 1-^{13}C-glycine (0.39 M) dispersed in a 60:40 water/glycerol solution containing 80mM 4-amino TEMPO. The spectra were recorded at 20K with (upper trace) and without (lower trace) microwave irradiation. A ^{1}H DNP enhancement of 170 ± 50 was observed with ~1.0 W of microwave power incident on the sample. Eight transients were recorded. The peak at ~75 ppm arises from glycerol at natural abundance.

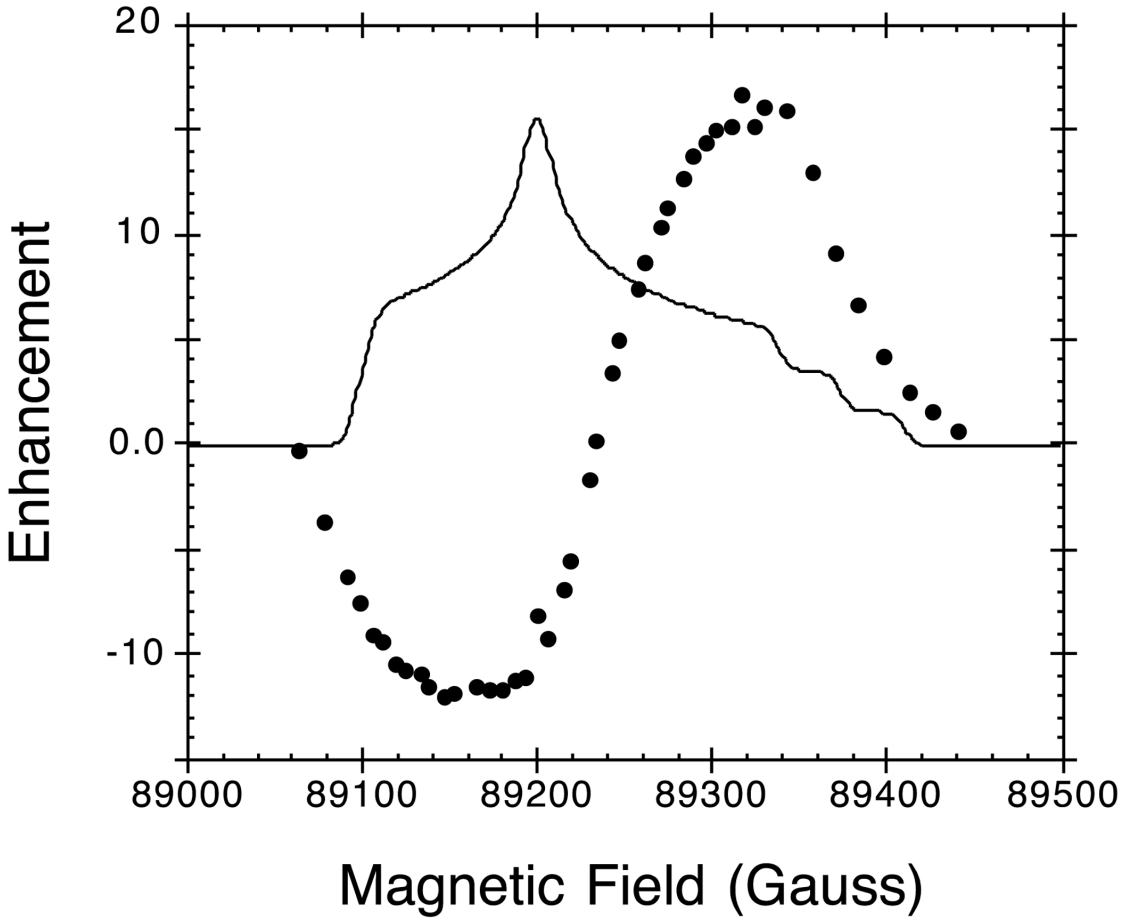

Fig. 3.

Dependence of the DNP enhancement (solid circles) on electron resonance offset, superimposed on the simulated 4-amino TEMPO EPR spectrum (solid trace). Because the gyrotron oscillator frequency is fixed, the static magnetic field was swept in this experiment. For the simulation of the TEMPO spectrum we employed g_{ii} and A_{ii} values from Budil et al. [30]; specifically, g_{xx} = 2.00860, g_{yy} = 2.00622, and g_{zz} = 2.00233 and A_{xx} = 0.66 mT, $_{Ayy}$ = 0.52 mT and A_{zz} = 3.54 mT.

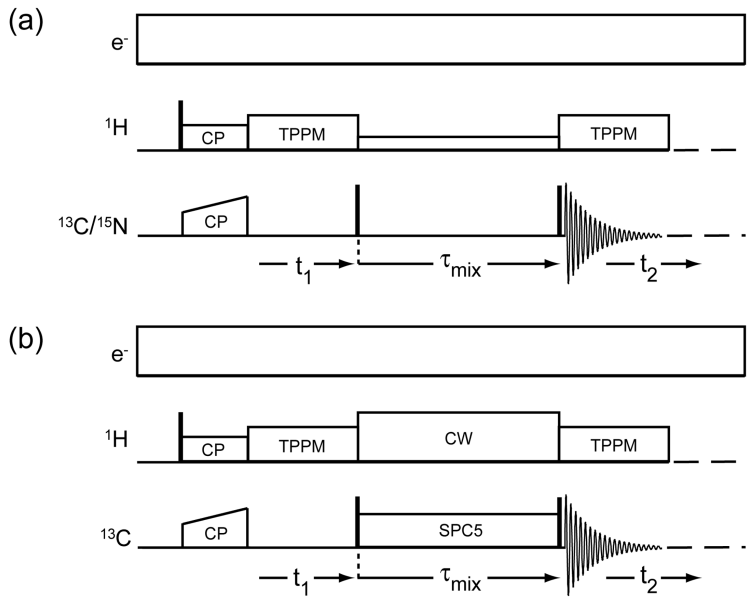

Fig. 4.

Sequences for two-dimensional homonuclear chemical shift correlation spectroscopy. Following cross polarization from $^{1}H–^{13}C$, the system evolves under the ^{13}C chemical shift for a period t_1. Correlations are established using mixing via: (a) proton-driven spin diffusion or (b) SPC5 homonuclear double-quantum mixing as described elsewhere [28,31], and detected during t_2.

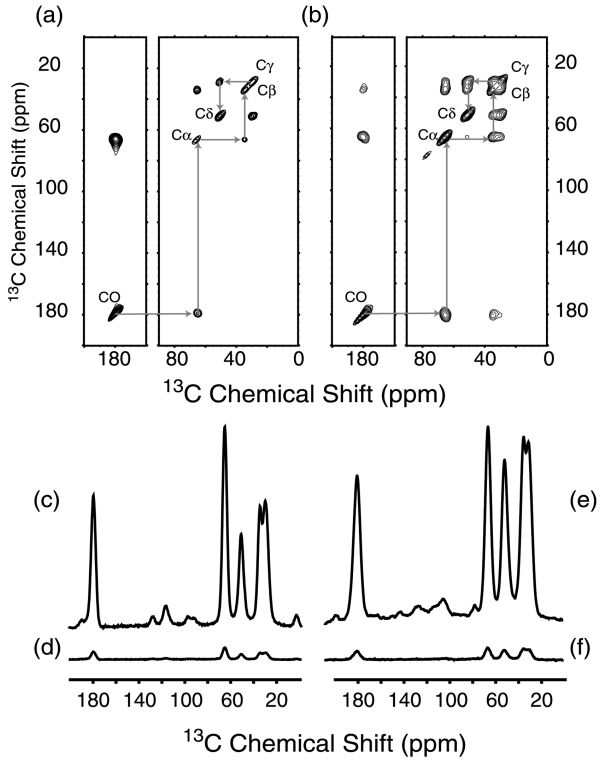

Fig. 5.

Two-dimensional ^{13}C–^{13}C correlation spectra of U-^{13}C, [^{15}N]proline, In (a), the SPC5 dipolar recoupling sequence was applied during a double quantum mixing period. The MAS frequency was 6 kHz, the mixing time was 1.33 ms, and the temperature was regulated at 97 ± 0.8 K. In (b), correlations were established by proton-driven spin diffusion for a mixing time of 10 ms. The MAS frequency was 7 kHz, and the temperature was unregulated but remained within the range 98–101 K. In both cases, 16 transients were acquired for each of 128 increments in the t_1 dimension, and the DNP enhancement was approximately 17. In (c) and (d), we show one dimensional ^{13}C MAS spectra obtained with and without DNP, respectively, using SPC5 recoupling with a double quantum phase cycle; (e) and (f) are CP spectra with and without DNP. The apparent intensity differences between the spectra in (c) and (e) are due to recoupling dynamics at short excitation times [31].